From Tetranuclear μ_4-Oxo to μ_4-Peroxocopper(II) Complexes

Jörg Reim, Rüdiger Werner, Wolfgang Haase, and Bernt Krebs*

Dedicated to Professor Achim Müller on the occasion of his 60th birthday

Abstract: The μ_4-peroxotetracopper(II) complexes $[Cu_4(L^1)_2(O_2)(OMe)_2(ClO_4)]$-$ClO_4 \cdot MeOH$ (**1**), $[Cu_4(L^2)_2(O_2)$-$(OMe)_2(ClO_4)]ClO_4 \cdot MeOH$ (**2**), $[Cu_4$-$(L^3)_2(O_2)(OMe)_2(ClO_4)]ClO_4 \cdot MeOH$ (**3**) and the μ_4-oxotetracopper(II) complex $[Cu_4(L^1)_2(O)(OH)_2(MeOH)_2$-$(ClO_4)_2]$ (**4**) were synthesized (HL^1 = 2,6-bis(pyrrolidinomethyl)-4-methylphenol, HL^2 = 2,6-bis(piperidinomethyl)-4-methylphenol, HL^3 = 2,6-bis(morpholinomethyl)-4-methylphenol). The molecular structures of **1** and **4** were established by single-crystal X-ray crystallography. **1** crystallizes in the monoclinic space group $P2/n$, with $a = 14.797(8)$, $b = 11.007(7)$, $c = 15.434(10)$ Å, $\beta = 118.29°$, $V = 2214$ Å^3 (150 K) and $Z = 2$. Complex **4** crystallizes in the monoclinic space group $P2_1/n$, with $a = 11.498(2)$, $b = 13.311(3)$, $c = 14.794(3)$ Å, $\beta = 93.56(3)°$, $V = 2259.9$ Å^3 (213 K) and $Z = 2$. Electrospray ionization mass spectra of **1** and **4** in dichloromethane solution confirm that the tetranuclear structure is maintained in this solvent. The UV/Vis spectra of **1**–**3** in dichloromethane are dominated by a very strong absorption at about 390 nm with a shoulder around 420–440 nm interpreted as a superposition of a peroxo $\rightarrow Cu^{II}$ and a phenolate $\rightarrow Cu^{II}$ charge-transfer transition. A band at about 580 nm may be a superposition of d–d transitions and a second, less intense peroxo $\rightarrow Cu^{II}$ charge transfer. The frequencies of the O–O stretching vibrations of **1**–**3** were determined by FT Raman and resonance Raman experiments and found to be 878, 898 and 888 cm^{-1}, respectively. A frequency shift to 841 cm^{-1} is observed upon ^{18}O substitution in **1**. The tetranuclear copper(II) complexes **1** and **4** are strongly antiferromagnetically coupled. They possess $S = 0$ ground states separated from a triplet state by 510 and 720 cm^{-1}, respectively. Good fits result from a regular spin Hamiltonian as well as from the Bleaney–Bowers equation, which shows that only the two lowest-lying states are notably thermally populated. Magnetostructural correlations established for dimeric complexes are not easily transferable to these kinds of tetrameric complexes. Investigations in methanolic solution provide evidence that a tetranuclear μ_4-oxocopper(II) complex analogous to **4** can be converted into a tetranuclear μ_4-peroxocopper(II) complex analogous to **1**.

Keywords: copper · magnetic properties · peroxo complexes · Raman spectroscopy · tetranuclear complexes

Introduction

In the field of copper coordination chemistry the synthesis and characterization of peroxo complexes is of particular interest and is the subject of intensive research.[1] Copper–dioxygen complexes are suggested as key intermediates not only in enzymatic reactions, but also in catalytic synthetic oxidation reactions. On the one hand, peroxocopper(II) complexes may serve as bioinorganic model compounds for the active sites of dioxygen-binding and dioxygen-activating copper proteins. On the other hand, they can contribute to the development of efficient low-molecular weight catalysts for the oxidation of organic substances by O_2.

Since the beginning of the 1980s considerable progress has been made in modelling and in the characterization of discrete CuO_2 and Cu_2O_2 adducts.[2–5] This includes detailed descriptions of the kinetics and thermodynamics of their formation, as well as of their spectroscopic and structural properties. Most copper–dioxygen adducts have to be characterized as solution species in aprotic solvents at low temperatures and are thermally unstable. Only one X-ray structure of a mononuclear side-on superoxocopper(II) complex[3] and two of dinuclear μ-peroxocopper(II) complexes are available. The complex synthesized by Karlin et al.[4] consists of two mononuclear copper(II) units bridged by a *trans*-μ-1,2-peroxo ligand, while that synthesized by Kitajima et al.[5] contains a planar μ-η^2:η^2-peroxo group simulating the spectroscopic,

[*] Prof. Dr. B. Krebs, Dipl.-Chem. J. Reim
Anorganisch-Chemisches Institut der Universität Münster
Wilhelm-Klemm-Strasse 8, D-48149 Münster (Germany)
Fax: Int. code + (49) 251 83-38366
e-mail: krebs@uni-muenster.de
Prof. Dr. W. Haase, Dipl.-Ing. R. Werner
Institut für Physikalische Chemie der Technischen Universität Darmstadt
Petersenstrasse 20, D-64287 Darmstadt (Germany)

  0947-6539/98/0402-0289 $ 17.50+.25/0

magnetic and structural properties of oxyhemocyanin.[6] Only a few papers report peroxocopper complexes showing considerable stability at ambient temperature.[7]

Herein we report the synthesis and characterization of a novel structural type of peroxocopper(II) complex where the peroxo ligand is bound in an unusual μ_4-$(\eta^1)_4$ coordination mode. The complexes are extraordinarily stable and can be generated and isolated at room temperature. Furthermore we describe the synthesis and characterization of a tetranuclear μ_4-oxo precursor complex. Parts of these results have been communicated previously.[8]

Results and Discussion

Syntheses: The tridentate amino alcohol ligands 2,6-bis(pyrrolidinomethyl)-4-methylphenol (HL^1), 2,6-bis(piperidinomethyl)-4-methylphenol (HL^2) and 2,6-bis(morpholinomethyl)-4-methylphenol (HL^3) are readily available by means of a Mannich reaction according to a literature method.[9] On addition of either hydrogen peroxide or 3,5-di-*tert*-butylcatechol (3,5-DTBC) to a methanolic solution containing the ligand HL^1, two equivalents of copper(II) perchlorate and an excess of triethylamine dark green crystals of $[Cu_4(L^1)_2(O_2)(OMe)_2(ClO_4)]ClO_4 \cdot MeOH$ (**1**) are formed . Whereas in the former case hydrogen peroxide itself is the peroxide source, in the latter case peroxide is formed in situ by the reduction of O_2 catalyzed by the copper(II) complex present. The detailed reaction mechanism for this complex two-electron reduction remains to be identified. Alternatively, **1** can be made by reaction of copper(I) perchlorate with HL^1 under argon in basic methanol followed by exposure to air. The latter method has the disadvantage that the initially formed copper(I) complex is unstable and decomposes rapidly. Complexes $[Cu_4(L^2)_2(O_2)(OMe)_2(ClO_4)]ClO_4 \cdot MeOH$ (**2**) and $[Cu_4(L^3)_2(O_2)(OMe)_2(ClO_4)]ClO_4 \cdot MeOH$ (**3**) are accessible by analogous syntheses. Complex $[Cu_4(L^1)_2(O)(OH)_2(MeOH)_2(ClO_4)_2]$ (**4**) crystallizes upon treatment of two equivalents of $[Cu(ClO_4)_2] \cdot 6H_2O$ with HL^1 from a concentrated basic methanolic solution. Details of the crystallographic measurements of **1** and **4** are given in Table 1.

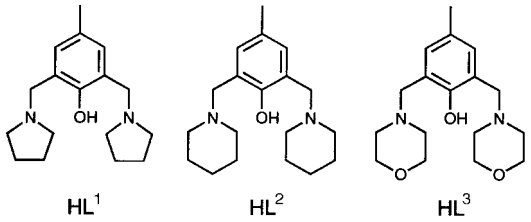

Table 1. Crystallographic data and experimental details of the structure determinations for compounds **1** and **4**.

	1	**4**
formula	$C_{37}H_{60}Cl_2Cu_4N_4O_{15}$	$C_{36}H_{60}Cl_2Cu_4N_4O_{15}$
M_r	1125.95	1113.94
crystal dimensions (mm)	$0.20 \times 0.12 \times 0.10$	$0.30 \times 0.25 \times 0.10$
crystal shape and colour	dark green prism	dark green plate
crystal system	monoclinic	monoclinic
space group	$P2/n$	$P2_1/n$
a (Å)	14.797(8)	11.498(2)
b (Å)	11.007(7)	13.311(3)
c (Å)	15.434(10)	14.794(3)
β (°)	118.29(4)	93.56(3)
V (Å^3)	2214	2259.9
Z	2	2
ρ_{calcd} (g cm^{-3})	1.689	1.637
$2\theta_{max}$ (°)	54.12	50.00
T (K)	150	213
measured reflections	5041	13784
unique reflections	4857	3941
observed reflections $[(I > 2\sigma(I)]$	2924	2018
refined reflections	4856	3840
parameters	290	290
R values $[(I > 2\sigma(I)]$ [a]	$R1 = 0.0357$, $wR2 = 0.0675$	$R1 = 0.0720$, $wR2 = 0.1399$
R values (all data) [a]	$R1 = 0.0763$, $wR2 = 0.0760$	$R1 = 0.1721$, $wR2 = 0.2015$
weighting scheme, w^{-1} [b]	$[\sigma^2(F_o^2) + (0.0246P)^2]$	$[\sigma^2(F_o^2) + (0.0377P)^2 + 18.4203P]$
residual electron density	0.52	0.61

[a] $R1 = \Sigma \,||F_o| - |F_c||/\Sigma\,|F_o|$, $wR2 = [\Sigma w(F_o^2 - F_c^2)^2/\Sigma w(F_o^2)^2]^{1/2}$. [b] $P = (F_o^2 + 2F_c^2)/3$.

Crystal structure of 1: The cation of **1** is shown in Figure 1 together with the atomic labelling system; selected interatomic distances and angles are given in Table 2. The molecule lies on a twofold crystallographic axis passing through the O2 – O2a peroxo group and Cl1 of the coordinating perchlorate anion. The peroxo ligand is bound end-on in a μ_4-$(\eta^1)_4$ coordination mode to four copper(II) ions that form a nearly planar rectangle. The peroxide is located above this rectangle resulting in a roof-like Cu_4O_2 geometry. The calculated distances of the peroxo group to the best Cu_4

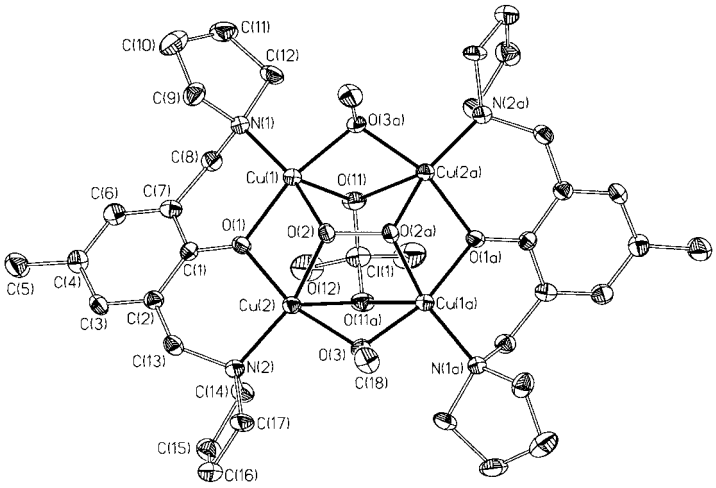

Figure 1. Molecular structure and atomic numbering scheme for the cation of **1** showing 50% probability thermal ellipsoids. Hydrogen atoms are omitted for clarity.

0947-6539/98/0402-0290 $ 17.50+.50/0 *Chem. Eur. J.* **1998**, *4*, No. 2

Table 2. Selected interatomic distances (Å) and angles (°) for **1**.[a]

Cu1 ··· Cu2	2.994(2)	Cu1 ··· Cu2a	3.030(2)
Cu1 ··· Cu1a	4.184(3)	Cu2 ··· Cu2a	4.317(2)
Cu1 – O1	1.939(2)	Cu2 – O1	1.941(3)
Cu1 – O2	1.961(2)	Cu2 – O2	1.939(2)
Cu1 – O3a	1.932(2)	Cu2 – O3	1.920(3)
Cu1 – O11	2.411(3)	Cu2 – O11a	2.693(3)
Cu1 – N1	2.006(3)	Cu2 – N2	1.986(3)
O2 – O2a	1.453(4)		
Cu1-O1-Cu2	101.0(1)	Cu1-O2-Cu2	100.3(1)
O1-Cu1-O2	76.2(1)	O1-Cu2-O2	76.6(1)
O1-Cu1-O3a	164.5(1)	O1-Cu2-O3	161.3(1)
O1-Cu1-O11	96.0(1)	O1-Cu2-O11 a	91.1(1)
O1-Cu1-N1	94.8(1)	O1-Cu2-N2	93.9(1)
O2-Cu1-O3a	88.9(1)	O2-Cu2-O3	91.3(1)
O2-Cu1-O11	96.8(1)	O2-Cu2-O11a	90.3(1)
O2-Cu1-N1	167.2(1)	O2-Cu2-N2	162.4(1)
O3a-Cu1-O11	81.5(1)	O3-Cu2-O11a	74.5(1)
O3a-Cu1-N1	100.6(1)	O3-Cu2-N2	101.2(1)
O11-Cu1-N1	93.2(1)	O11a-Cu2-N2	104.8(1)
Cu1-O2-O2a	113.7(2)	Cu2-O2-O2a	113.8(2)

[a] Symmetry transformation for equivalent atoms: $-x+0.5$, y, $-z+0.5$.

plane are 1.008(2) and 1.078(2) Å for O2 and O2a, respectively. Cu1 and Cu2 (as well as Cu1a and Cu2a) are bridged by the phenoxo group of the deprotonated ligand $(L^1)^-$ and are each terminally coordinated by the pyrrolidine groups of the ligand. Cu1 and Cu2a (as well as Cu2 and Cu1a) are bridged by a methanolato group. Below the Cu_4 rectangle a perchlorate group is bound to all four metal centres through O11 (to Cu1 and Cu2a) and O11a (to Cu2 and Cu1a). The perchlorate oxygen atoms occupy the apices of the square-pyramidal Jahn–Teller distorted coordination spheres of the copper centres.

The μ_4 coordination mode is very unusual and has been observed only in $[Fe_6(O)_2(O_2)(O_2CPh)_{12}(OH_2)_2]$,[10] $K_4[Mo_4O_{12}(O_2)_2]$,[11] $[Fe_6(O)_2(O_2)_3(OAc)_9]^{-}$[12] and $[(o\text{-}Tol\text{-}SbO)_4(O_2)_2]$.[13] While in the case of the first-mentioned example the peroxide is bound in plane with the metals, in **1** as well as in the other three compounds the O_2^{2-} group lies above the corresponding M_4 plane. The μ_4-O_2^{2-} unit is discussed as a potential intermediate in the oxidation of water to O_2 by the tetranuclear Mn complex of photosystem II.[14] This structural motif is also under discussion for the catalytic dismutation of H_2O_2 by a tetranuclear Mn complex[15] and for the thermal decomposition of dinuclear μ-peroxodiiron(III) complexes.[16]

Crystal structure of 4: The molecular structure of **4** is depicted in Figure 2 along with the atomic numbering scheme. Figure 3 shows thermal ellipsoids of the asymmetric unit. Relevant interatomic distances and angles are given in Table 3. The complex consists of a rectangle of four Cu^{II} atoms coordinating to a central μ_4-oxygen atom lying on a crystallographic inversion centre. Thus, for symmetry reasons the central Cu_4O core is exactly planar. Each of two opposite sides are bridged by a hydroxo group (Cu1 – Cu2a, Cu2 – Cu1a) and a μ-phenoxo group (Cu1 – Cu2, Cu1a – Cu2a) of the deprotonated ligand $(L^1)^-$. Each metal is coordinated by a pyrrolidine nitrogen atom of the ligand $(L^1)^-$, which completes the basal planes of the copper coordination spheres. The hydroxo-bridged copper units are further bridged by two axially coordinating ligands, one perchlorate anion and a disordered

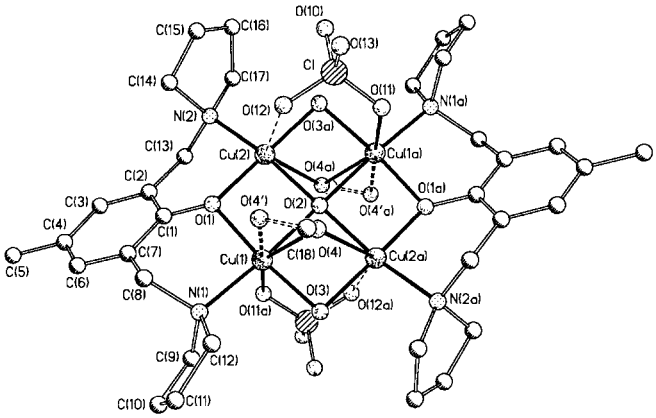

Figure 2. Molecular structure and atomic numbering scheme for **4**. Hydrogen atoms are omitted for clarity.

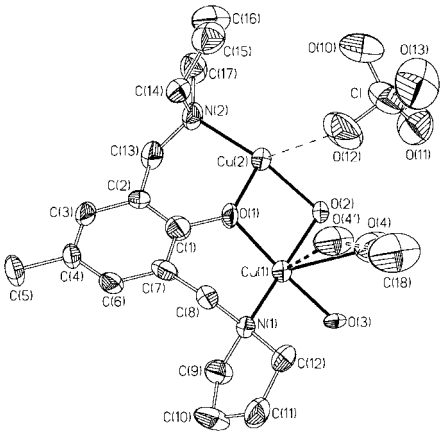

Figure 3. Asymmetric unit of **4** showing 50% probability thermal ellipsoids.

Table 3. Selected interatomic distances (Å) and angles (°) for **4**.[a]

Cu1 ··· Cu2	2.862(2)	Cu1 ··· Cu2a	2.749(2)
Cu1 – O1	1.880(6)	Cu2 – O1	1.927(6)
Cu1 – O2	2.022(1)	Cu2 – O2	1.945(1)
Cu1 – O3	1.879(7)	Cu2 – O3a	1.881(6)
Cu1 – O4	2.686(15)	Cu2 – O4a	2.819(19)
Cu1 – O4′	2.694(28)		
Cu1 – O11a	2.808(9)	Cu2 ··· O12	3.295(12)
Cu1 – N1	2.084(8)	Cu2 – N2	1.958(7)
Cu1-O1-Cu2	97.5(3)	Cu1-O2-Cu1a	180.0
Cu1-O2-Cu2a	87.7(1)	Cu1-O2-Cu2	92.3(1)
Cu2-O2-Cu2a	180.0	Cu1-O3-Cu2a	94.0(3)
Cu1-O4-Cu2a	59.9(3)	O1-Cu1-O2	84.5(2)
O1-Cu1-O3	169.7(3)	O1-Cu1-O4	107.2(5)
O1-Cu1-O4′	86.4(9)	O1-Cu1-O11a	91.5(3)
O1-Cu1-N1	93.4(3)	O2-Cu1-O3	87.1(2)
O2-Cu1-O4	74.9(4)	O2-Cu1-O4′	92.7(9)
O2-Cu1-O11a	86.3(2)	O2-Cu1-N1	172.5(2)
O3-Cu1-O4	76.2(5)	O3-Cu1-O4′	99.9(10)
O3-Cu1-O11a	82.0(3)	O3-Cu1-N1	95.7(3)
O4-Cu1-O11a	151.7(5)	O4-Cu1-N1	99.0(5)
O4′-Cu1-O11a	177.7(7)	O4′-Cu1-N1	80.0(9)
O11a-Cu1-N1	101.0(3)	O1-Cu2-O3a	164.3(3)
O1-Cu2-O2	85.4(2)	O1-Cu2-N2	92.2(3)
O2-Cu2-O3a	89.3(2)	O2-Cu2-N2	167.2(2)
O3a-Cu2-N2	96.2(3)		

[a] Symmetry transformation for equivalent atoms: $-x$, $-y$, $-z+1$.

methanol molecule. However, in the less occupied site the methanol serves as a terminal ligand (through O4′) to Cu1. The Cu–O bond lengths in the μ-hydroxo bridges are remarkably short (see Table 3), while all other equatorial bond lengths have normal values.

The structures of **1** and **4** are closely related. Complex **4** can be regarded as the precursor complex for the synthesis of **1** (vide infra). Compound **4** contains an oxo anion instead of the peroxo group and hydroxo instead of methanolato bridges. Whereas the peroxo ligand in **1** is positioned above the Cu_4 rectangle, the oxo ligand in **4** is located in the plane with the metal centres; this causes a shortening of the metal–metal distances. The μ-phenoxo-bridged copper atoms move together from 2.994(2) to 2.862(2) Å, for the μ-hydroxo-bridged copper centres this effect is even more drastic with a reduction from 3.030(2) to 2.749(2) Å. To our knowledge, besides compound **4** only one other complex has been reported with an exactly planar $Cu_4(\mu_4\text{-O})$ unit. In the heteronuclear complex $[Cu_4Zr_4O_3(O\mathit{i}Pr)_{18}]$ the isopropylato bridged copper centres exhibit similiar short Cu–Cu distances of 2.781(8) Å.[17] The structure of the complex $[Cu_4(\mu_4\text{-OH})L^4]^{3+}$ (L^4 = macrocyclic Schiff-base ligand) is very similiar to that of **4**, but instead of an oxo anion a (disordered) hydroxide is located on the inversion centre.[18] However, on deprotonation of the hydroxide in aprotic solvents dimerization to the octanuclear complex $[\{Cu_4(\mu_5\text{-O})L^4(ClO_4)\}_2]^{2+}$ is observed, in which the O^{2-} is displaced from the central Cu_4 plane towards the additionally coordinated copper.[18] The Cu–Cu distances within the tetranuclear subunit lie in the same range as in **4**: the alkoxo-bridged metal centres have interatomic distances of 2.85 Å (averaged), the phenoxo-bridged centres 2.90 Å (averaged).

While tetranuclear copper(II) complexes involving a planar $\mu_4\text{-}O^{2-}$ unit are rare, numerous copper(II) complexes containing a (distorted) μ_4-oxo bridge have been described.[19] In the presence of coordinating anions such as halides or carboxylates tetrahedral μ_4-oxocopper(II) complexes are the preferred products when tridentate amino alcohol ligands of the type used in this work are employed.[19a–c] In these compounds the copper centres of each dinuclear subunit are bridged unsymmetrically giving rise to one short equatorial and one long axial Cu–X bond length (X = halide, carboxylate); the metal–metal bond lengths range from 3.15 to 3.38 Å. In the synthesis of **4** only hydroxide or methanolate ions are available to serve as coordinating anions. Their bite distance is probably too short for the described bridging mode and therefore they are not able to stabilize the tetrahedral arrangement of the four copper ions around the central oxo anion.

UV/Vis spectroscopic properties: The spectra of complexes **1**–**4** were recorded in dichloromethane in the range 250–1000 nm. The concentrations used were 10^{-4} mol L^{-1}, except for **3,** for which a 6×10^{-5} mol L^{-1} solution was prepared on account of its poor solubility. Dichloromethane is a very weakly coordinating solvent, so the tetranuclear structures of the complexes are maintained in dichloromethane solution, as is indicated by electrospray ionization mass spectrometry (vide infra). Figure 4 displays the UV/Vis spectra of **1** and **4** in the range 300–800 nm and Table 4 contains the exact data for all of the complexes.

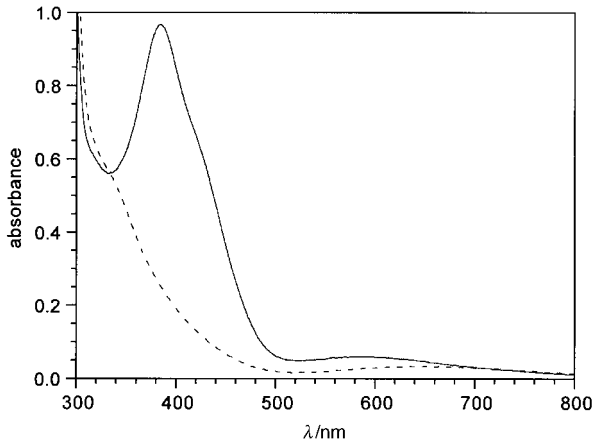

Figure 4. UV/Vis spectra of **1** (solid line) and **4** (dashed line) in dichloromethane ($c = 10^{-4}$ mol L^{-1}).

Table 4. UV/Vis data of complexes **1**–**4**.

	λ(nm)	ε (M^{-1}cm^{-1})	λ (nm)	ε (M^{-1}cm^{-1})	λ (nm)	ε (M^{-1}cm^{-1})
1	284	15900	384	9700	587	610
2	287	16200	389	9500	586	580
3	287	16600	391	9300	565	770
4	270–280 (sh)	–	320–440 (sh)	–	645	340

The bands near 290 nm are attributed to $\pi\rightarrow\pi^*$ transitions within the ligands. As expected, all three peroxo complexes exhibit similar band structures. The spectra are dominated by a very strong absorption at about 390 nm with a shoulder around 420–440 nm. In this region no distinct band is observed for **4,** but there is a broad shoulder in the range 320–440 nm attached to the inner ligand band. This is attributed to a phenolate $\rightarrow Cu^{II}$ charge-transfer transition. Hence, the band structure in the spectra of the peroxo compounds can be interpreted as a superposition of a peroxo $\rightarrow Cu^{II}$ and a phenolate $\rightarrow Cu^{II}$ charge-transfer transition. The band at about 580 nm seems to be too high in energy for pure d–d transitions and may be superposed on a second, less intense peroxo $\rightarrow Cu^{II}$ charge transfer (even for a simple mononuclear peroxocopper(II) complex two peroxo $\rightarrow Cu^{II}$ charge-transfer transitions are predicted[20]). The maximum of the d–d bands of **4** is located at 645 nm as expected for square-pyramidal copper(II) ions.[21]

Electrospray ionization mass spectrometry (ESI-MS): ESI-MS spectra of solutions of **1** and **4** in dichloromethane were recorded. Besides some minor peaks, the mass spectrum of the solution of **4** essentially contains one peak pattern with the intensity maximum at m/z 949. Since the theoretical isotopic pattern is in excellent agreement with the experimental one these peaks can be assigned to the cation $[Cu_4(L^1)_2(O)(OH)_2]^{2+}(ClO_4)^-$. The spectrum of the solution of **1** shows six peak patterns in the range m/z 900–1000 with intensity maxima at m/z 915, 930, 949, 965, 979 and 993. On the basis of

0947-6539/98/0402-0292 $ 17.50+.50/0 *Chem. Eur. J.* **1998**, *4*, No. 2

the theoretical isotope distributions the latter pattern indicates the presence of $[Cu_4(L^1)_2(O_2)(OCH_3)_2]^{2+}(ClO_4)^-$. The peaks at *m/z* 979 and 965 can be assigned if a consecutive exchange of methanolate by hydroxide is assumed, and leads to the formulae $[Cu_4(L^1)_2(O_2)(OCH_3)(OH)]^{2+}(ClO_4)^-$ and $[Cu_4(L^1)_2(O_2)(OH)_2]^{2+}(ClO_4)^-$, respectively. The peak at *m/z* 915 can be assigned to species such as $[Cu_4(L^1)_2(O_2)(OCH_3)(OH)_2(H_2O)]^+$ or $[Cu_4(L^1)_2(O_2)(OH)_3(CH_3OH)]^+$. Also in these cases the theoretical isotopic patterns in the mass spectra are in accordance with the experimental ones. The water present in the dichloromethane solvent as a contaminant can exchange with the less polar methanol in the complex. The peak pattern at *m/z* 949 in the ESI mass spectrum of the solution of **1** corresponds to that of **4**, so **4** is most probably present as an impurity in the sample of **1**. The peak at *m/z* 930 cannot be definitively ascribed to one particular species.

Vibrational spectroscopy: The identification of $\tilde{\nu}$(O–O) of peroxocopper(II) complexes is of major interest. For this purpose **1** was also prepared with $^{18}O_2$, yielding an isotopic labelled derivative **1-^{18}O**. Besides routine IR spectra, peroxo complexes **1**, **1-^{18}O**, **2** and **3** were studied by FT Raman and resonance Raman spectroscopy. The FT Raman spectra were recorded at room temperature, while the resonance Raman experiments were performed at low temperature with laser excitation from 514.5 to 454.5 nm. Figure 5 shows the resonance Raman spectra of **1** and **1-^{18}O**, Figure 6 depicts the respective FT Raman spectra and Table 5 gives a summary of the observed frequency shifts of complex **1** upon ^{18}O substitution in various experiments.

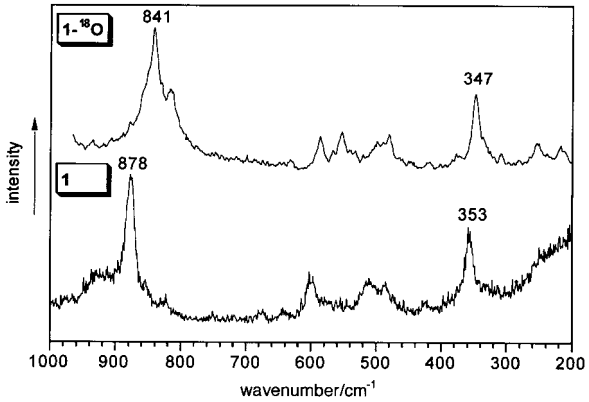

Figure 5. Resonance Raman spectra of **1** (457.9 nm, 10 K) and **1-^{18}O** (454.5 nm, 80 K).

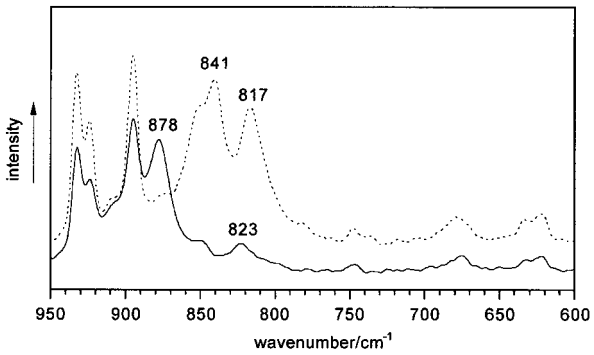

Figure 6. FT Raman spectra (950–600 cm^{-1}) of **1** (solid line) and **1-^{18}O** (dashed line).

Table 5. Observed frequency shifts (cm^{-1}) of **1** upon ^{18}O substitution in resonance Raman (RR), Raman (R) and IR spectroscopic (IR) investigations.

1	**1-^{18}O**	Observed in
878	841	RR/R
823	817	R
388	384	IR
353	347	RR/R/IR
331	329	IR
316	306	IR

The resonance Raman spectra of **1** and **1-^{18}O** each contain two strong bands at 878 and 353 cm^{-1}, and 841 and 347 cm^{-1}, respectively; the spectra were recorded with excitation at 457.9 and 454.5 nm , respectively. Measurements performed with excitation up to 514.5 nm were very similar. In the FT Raman spectra, shifts of three bands are observed upon isotopic substitution. The bands at 878, 823 and 353 cm^{-1} shift to 841, 817 and 347 cm^{-1}, respectively. The IR spectra (4000–450 cm^{-1}) of **1** and **1-^{18}O** are identical, but in the FIR region significant shifts are noted (listed in Table 5). The band at 878 cm^{-1} can be assigned definitively to $\tilde{\nu}$(O–O) while the 353 cm^{-1} band is attributed to a Cu–O peroxide vibration. If the peroxo group is considered as a harmonic diatomic oscillator, theoretical values for the isotopic labelled compound of 828 and 338 cm^{-1} are expected. Obviously, the observed frequencies deviate significantly, revealing clear nonharmonic behaviour. A further indication of vibrational couplings within the central Cu_4 core is the shift of the band at 823 to 817 cm^{-1} in the FT Raman spectrum.

In the resonance Raman spectra of **2** and **3** two characteristic Raman features are also found which are correspondingly assigned to the O–O stretching vibration and a Cu–O peroxide vibration. Whereas the frequencies of the metal–donor vibrations are essentially identical (353, 352 and 353 cm^{-1} in **1**, **2** and **3**, respectively) for all three peroxo complexes, the peroxide vibrations differ remarkably (878, 898 and 888 cm^{-1} in **1**, **2** and **3**, respectively).

Table 6 contains O–O stretching vibrations and O–O bond lengths of structurally and/or spectroscopically characterized peroxocopper(II) complexes, of type 3 copper proteins and of μ_4-peroxoiron(III) complexes. It is evident that the stretching vibrations of peroxocopper(II) complexes and proteins can be classified into three groups: compounds containing μ-η^2:η^2 bound peroxide exhibit the lowest values for $\tilde{\nu}$(O–O) (731–755 cm^{-1}),[5,6c,22,23] tetranuclear complexes **1**–**3** featuring the μ_4-coordinated peroxide have the highest values (878–898 cm^{-1}) whereas the *trans*-μ-1,2 complex[4,24] and the complex with the terminal peroxide[25] give values in between (832 and 803 cm^{-1}, respectively). Hence, the comparatively high O–O stretching frequencies of the μ_4-peroxocopper(II) complexes are unique and can be considered

Table 6. O–O stretching vibration frequencies and O–O bond lengths of selected peroxo compounds.

	coordination mode	$\tilde{\nu}$(O–O) (cm^{-1})	d(O–O) (Å)	ref.
$[Cu\{HB(3,5\text{-}Me_2pz)_3\}]_2(O_2)$ [a]	μ-η^2:η^2	731		[22]
$[Cu(HB(3,5\text{-}iPr_2pz)_3]_2(O_2)$	μ-η^2:η^2	741	1.412(12)	[5]
$[Cu(HB(3,5\text{-}Ph_2pz)_3]_2(O_2)$	μ-η^2:η^2	759		[5]
oxyHc	μ-η^2:η^2	742–752		[6c, 23a–e]
oxyTyr	μ-η^2:η^2	755		[23f]
$[Cu_2(XYL-O\text{-})(O_2)]^+$	terminal	803		[25]
$[\{Cu(tpa)\}_2(O_2)]^{2+}$	*trans*-μ-1,2	832	1.432(6)	[4,24]
1	μ_4	878	1.453(4)	this work
2	μ_4	898		this work
3	μ_4	888		this work
$[Fe_6(O)_2(O_2)(O_2CPh)_{12}(OH_2)_2]$	μ_4	853	1.480(12)	[10]
$[Fe_6(O)_2(O_2)_3(OAc)_9]^-$	μ_4	844	1.472(9)	[12]

[a] pz = pyrazolyl.

as a spectroscopic characteristic of this class of compounds. The O–O stretching vibrations of the copper compounds correlate nicely with the observed O–O bond lengths (Table 6). However, the $\tilde{\nu}$(O–O) values of the μ_4-peroxo-iron(III) complexes[10,12] do not fit into this scheme. Despite the iron complexes having the same coordination mode, the O–O bonds are longer and the $\tilde{\nu}$(O–O) values are lower than in the corresponding copper complexes.

Magnetic properties: Magnetic susceptibility measurements on polycrystalline samples of **1** and **4** were made in the temperature range 6.0–411.2 K for **1** and 4.3–401.8 K for **4**. The magnetic moments of both complexes decrease with decreasing temperature whereas the magnetic susceptibilities show minima at 80 K (**1**) and 170 K (**4**). The room-temperature values for μ_{eff} per copper centre are 0.80 μ_B for **1** and 0.65 μ_B for **4**. These values are lower than the spin-only value of 1.73 μ_B for a copper(II) ion; this means that both complexes are strongly antiferromagnetically coupled. In Figures 7 and 8 plots of the susceptibilities and the effective magnetic moments versus temperature are shown.

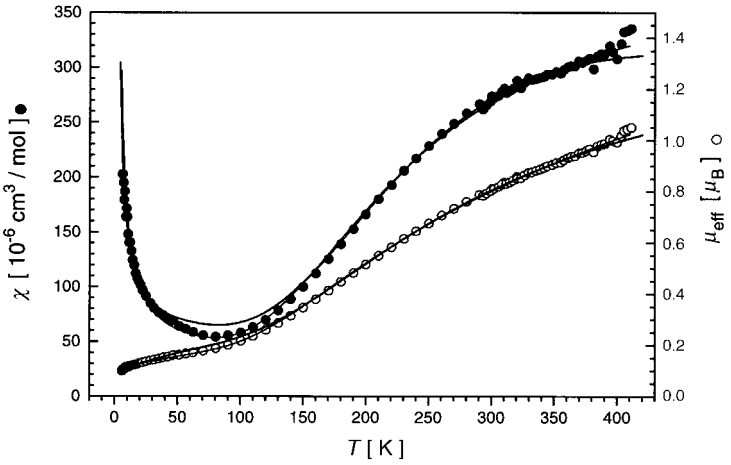

Figure 7. Molar susceptibility and effective magnetic moment per copper atom of **1**. Lower curve in each plot: fit with Equation (3); upper curve in each plot: fit with Equation (8).

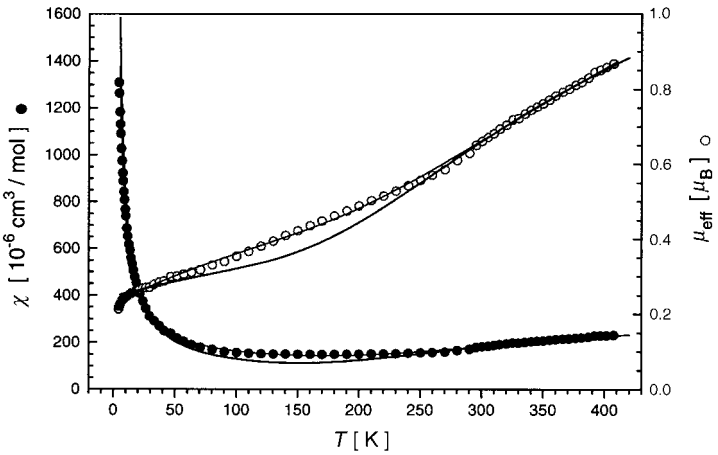

Figure 8. Molar susceptibility and effective magnetic moment per copper atom of **4**. Lower curve in each plot: fit with Equation (3); upper curve in each plot: fit with Equation (4).

For theoretical calculations an isotropic Heisenberg approach can be used based on the common spin-exchange Hamiltonian [Eq. (1)].

$$\hat{H} = -2\sum_{ij} J_{ij}\hat{\mathbf{S}}_i\hat{\mathbf{S}}_j \quad (1)$$

As a result of the the C_i symmetry of complex **4** three different coupling constants J_{12}, J_{13}, and J_{14} have to be taken into account (Scheme 1). The Hamiltonian of the tetranuclear system in this case is given in Equation (2).

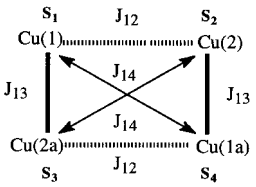

Scheme 1. Exchange coupling model for **1** and **4**.

$$\hat{H} = -2J_{12}(\hat{\mathbf{S}}_1\hat{\mathbf{S}}_2 + \hat{\mathbf{S}}_3\hat{\mathbf{S}}_4) - 2J_{13}(\hat{\mathbf{S}}_1\hat{\mathbf{S}}_3 + \hat{\mathbf{S}}_2\hat{\mathbf{S}}_4) - 2J_{14}(\hat{\mathbf{S}}_1\hat{\mathbf{S}}_4 + \hat{\mathbf{S}}_2\hat{\mathbf{S}}_3) \quad (2)$$

Because of the C_2 symmetry of complex **1** a correct model of this arrangement of spin centres must have four different coupling constants. However, since the chemical conditions of the two diagonal pathways are identical, the coupling scheme used for compound **4** should be valid [Eq. (2)].

Diagonalization of the spin matrix with the basis set $\langle S_{12},S_{34},S|$ leads to an analytical expression for the energy eigenvalues that can be inserted into van Vleck's equation. The resulting expression for the temperature dependence of the magnetic susceptibility is given in Equation (3); χ_{tetra}, χ_{imp}, A and B are defined in Equations (4–7), respectively, S = 1/2 and N_A, μ_B, h, k, c and g have their usual meaning and x_{imp} is the percentage of susceptibility caused by paramagnetic impurity.

$$\chi(T) = (1 - x_{imp}) \times \chi_{tetra}(T) + 4x_{imp}\chi_{imp}(T) + 4N_\alpha \quad (3)$$

$$\chi_{tetra}(T) = \frac{N_A g^2 \mu_B^2}{3kT} \times \frac{A}{B} \quad (4)$$

$$\chi_{imp}(T) = \frac{N_A g^2 \mu_B^2}{4kT} \quad (5)$$

0947-6539/98/0402-0294 $ 17.50+.50/0 *Chem. Eur. J.* **1998**, *4*, No. 2

$$A = 30\exp\left(-\frac{(-J_{12}-J_{13}-J_{14})hc}{kT}\right)+6\exp\left(-\frac{(J_{12}+J_{13}-J_{14})hc}{kT}\right)+6\exp\left(-\frac{(J_{12}-J_{13}+J_{14})hc}{kT}\right)+6\exp\left(-\frac{(-J_{12}+J_{13}+J_{14})hc}{kT}\right) \quad (6)$$

$$B = 5\exp\left(-\frac{(-J_{12}-J_{13}-J_{14})hc}{kT}\right)+3\exp\left(-\frac{(J_{12}+J_{13}-J_{14})hc}{kT}\right)+3\exp\left(-\frac{(J_{12}-J_{13}+J_{14})hc}{kT}\right)+3\exp\left(-\frac{(-J_{12}+J_{13}+J_{14})hc}{kT}\right)$$
$$+\exp\left(-\frac{\left(J_{12}+J_{13}+J_{14}-2\sqrt{J_{12}^2+J_{13}^2+J_{14}^2-J_{12}J_{13}-J_{12}J_{14}-J_{13}J_{14}}\right)hc}{kT}\right)+\exp\left(-\frac{\left(J_{12}+J_{13}+J_{14}+2\sqrt{J_{12}^2+J_{13}^2+J_{14}^2-J_{12}J_{13}-J_{12}J_{14}-J_{13}J_{14}}\right)hc}{kT}\right) \quad (7)$$

For a quantitative description of the magnetic properties of the tetranuclear compounds examined the data were fitted for molar susceptibility versus temperature by means of Equation (3). Unfortunately, for both systems a satisfying fit could not be obtained. Particularly in the temperature region between 50 and 250 K, the fits are not good when the estimated values of diamagnetic susceptibility and the standard value of 60×10^{-6} cm^3 mol^{-1} for N_α are used. Owing to the strong antiferromagnetic coupling, the absolute values of the molar susceptibility are very low. In this case the estimation of the diamagnetic correction becomes very important. Assuming a maximal error of estimation of 10 %, the influence of this parameter on the overall susceptibility and on the fits is remarkable. A variation of temperature-independent paramagnetism (TIP) has the same effect on susceptibility. Therefore fits with variable TIP were made. The results, which were much more satisfying, are shown in Figures 7 and 8.

A fit for complex **1** with Equation (3) leads to $g = 2.07$, $x_{imp} = 0.11$ % and $N_\alpha = 35 \times 10^{-6}$ cm^3 mol^{-1}. Surprisingly, this fit does not lead to reproducible values for any of the three J_{ij}. As a consequence of the strong antiferromagnetic coupling only the $S = 1$ first excited state, besides the $S = 0$ ground state, is thermally accessible at temperatures up to $\approx$400 K. Consequently the tetrameric complex can be described magnetically by a two-energy-state model with nearly the same level of accuracy. Therefore Equation (2) was substituted by the well-known Bleaney–Bowers equation [Eq. (8)].[26] This treatment leads to a nearly identical fit (upper curves in Figure 7) with $2J = -510 \pm 20$ cm^{-1}, which is good confirmation that in magnetic susceptibility measurements only the first singlet–triplet gap is accessible.

$$\chi = \frac{2N_A g^2 \mu_B^2}{kT} \times \frac{\exp\left(\frac{2J}{kT}\right)}{1+3\exp\left(\frac{2J}{kT}\right)} \quad (8)$$

All the facts described above are valid for compound **4** too. This complex is very strongly antiferromagnetically coupled; the fitting procedure with the Bleaney–Bowers equation results in $2J = -720 \pm 60$ cm^{-1}. In Figure 8 the upper lines belong to the best fit of Equation (8), while the lower lines represent the best fit of Equation (3) with $g = 2.19$, $x_{imp} = 0.47$ % and $N_\alpha = 98 \times 10^{-6}$ cm^3 mol^{-1}.

For dinuclear Cu^{II} complexes a number of magnetostructural correlations have been established in the last 20 years.[19a,27,28] All these correlations show a strong linear dependency of the exchange integral on the bridging angle at the diamagnetic oxygen atom. In all cases the bridging angle at the point where the sign of the exchange interaction changes is nearly the same, namely $97.5 \pm 1.0°$. For smaller angles, ferromagnetic interactions are found. In **1** the Cu-O-Cu angles are larger than 100.0°. Therefore, if magnetostructural correlations made for square-planar dinuclear copper(II) complexes can be applied to this kind of tetranuclear complex, antiferromagnetic interactions would be expected. A prediction of the interaction through the peroxo bridge is much more complicated. No correlation exists for this structural unit. A comparable structural motif is present in the *trans*-μ-1,2-peroxocopper(II) complex $[\{Cu(tpa)\}_2(O_2)]^{2+}$.[4] In spite of the large Cu···Cu interatomic distance of 4.359(1) Å, which is similar to the 4.25 Å (averaged) in **1,** a strong antiferromagnetic exchange coupling including the copper d_{z^2} orbitals of $-2J > 600$ cm^{-1} is found.[29]

In the case of **4** most bridging angles are smaller than 97.5°; thus ferromagnetic interaction could be expected. However, the measured susceptibilities show clearly that for this kind of tetrameric complex a simple transfer of the known correlations for dimeric complexes is not possible. Contrary to the predictions at least one of the nondiagonal interactions is strongly antiferromagnetic. It should be noted that all predictions and correlations are based upon a superexchange mechanism. Owing to the very short copper–copper distances in this complex (2.75 and 2.86 Å) direct exchange should also be taken into account as it would enforce the observed antiferromagnetic interaction. For both complexes an unambiguous assignment of exchange parameters to structure units is difficult to formulate.

Investigation of the system in solution: The μ_4-peroxo complexes **1**–**3** can be synthesized in methanol on treatment of the corresponding tridentate ligand HL^1, HL^2 or HL^3 with two equivalents of copper(II) perchlorate, triethylamine and hydrogen peroxide or 3,5-DTBC/O_2. Two dinuclear $Cu_2(L)^{3+}$ units ($L = (L^1)^-$, $(L^2)^-$, $(L^3)^-$) need to dimerize to give the tetranuclear species with additional coordination of one peroxide group, two methanolate groups and one perchlorate anion. To achieve further insight into this complex reaction system we studied the species in solution by UV/Vis spectroscopy.

A methanolic solution containing the ligand HL^1 (2×10^{-4} mol L^{-1}) and copper(II) perchlorate hexahydrate (4×10^{-4} mol L^{-1}) (simplified as Cu_2L^1 with $c = 2 \times 10^{-4}$ mol L^{-1}) was titrated with NEt_3 spectrophotometrically. A uniform increase of the bands in the UV/Vis spectrum on addition of the first three equivalents (per Cu_2L^1) suggests quantitative formation of the complex from the ligand and metal ions, where the base may be used for deprotonation of the endogenous phenol bridging group and an exogenous bridging solvent molecule. The maximum of the d–d bands is observed at about 685 nm with $\varepsilon = 230$ M^{-1} cm^{-1} (per Cu_2L^1). Further addition of base leads to a change of the form of the

spectrum. The practical end-point of the titration is reached after addition of about 30 equivalents of NEt_3. The d – d bands shift to 650 nm with concomitant decrease of intensity ($\varepsilon = 170\,M^{-1}cm^{-1}$ per Cu_2L^1). The spectrum obtained is very similar to that of **4** in dichloromethane (see Figure 4) and nearly identical to that of **4** recorded in methanol. In this basic medium a reaction is proposed whereby a tetranuclear μ_4-oxo species is formed, with a structure analogous to **4** in the solid state.

A solution of Cu_2L^1 (2×10^{-4} mol L^{-1}) in methanol to which 30 equivalents of NEt_3 have been added was titrated with hydrogen peroxide. The recorded spectra are depicted in Figure 9. In the course of the titration a new charge-transfer

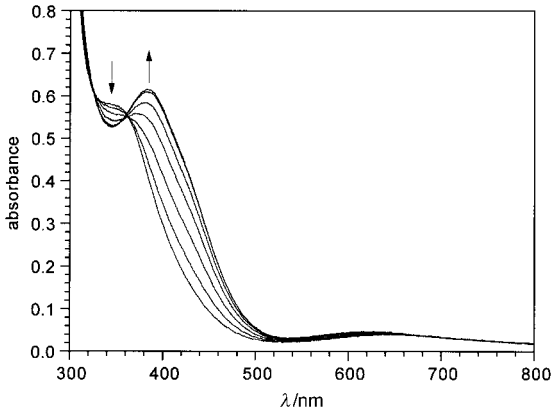

Figure 9. UV/Vis spectra from the titration of Cu_2L^1 (2×10^{-4} mol L^{-1} in methanol) + 30 equivalents of triethylamine with 0.25, 0.5, 0.75, 1.0, 1.25 and 1.5 equivalents of H_2O_2.

band with a maximum at 383 nm develops. Two isosbestic points at 325 and 363 nm indicate an equilibrium between two complexes; the maximum of the d – d bands shifts from about 650 to 620 nm. The end of the transformation is reached after addition of 1.5 equivalents per Cu_2L^1 and 3 equivalents per tetranuclear unit. The similarity of the obtained UV/Vis spectrum to that of the μ_4-peroxocopper(II) complex **1** in dichloromethane is apparent. Both spectra have a maximum at nearly the same wavelength in the charge-transfer region (384 nm (**1**) and 383 nm). However, the extinction coefficients differ significantly with $\varepsilon = 9700\,M^{-1}cm^{-1}$ (**1**) and $\varepsilon = 6200\,M^{-1}cm^{-1}$ (per Cu_4 unit). A further difference is seen in the visible region of the spectra. For **1** the maximum is found at 587 nm ($\varepsilon = 610\,M^{-1}cm^{-1}$); for the complex formed in the titration the band is located at 620 nm ($\varepsilon = 450\,M^{-1}cm^{-1}$ per Cu_4 unit).

It is evident that in basic methanolic solution a tetranuclear μ_4-oxocopper(II) complex can be converted into a tetranuclear μ_4-peroxocopper(II) complex by addition of H_2O_2 or 3,5-DTBC/O_2 (Scheme 2). The differences in the spectra of the in situ synthesized peroxo complex in methanol and of the dissolved crystalline peroxo complex **1** in dichloromethane are probably a result of solvent effects. Whereas methanol is a strongly coordinating solvent, dichloromethane has only weakly coordinating properties. Thus additional coordination of the solvent molecules may influence the charge-transfer

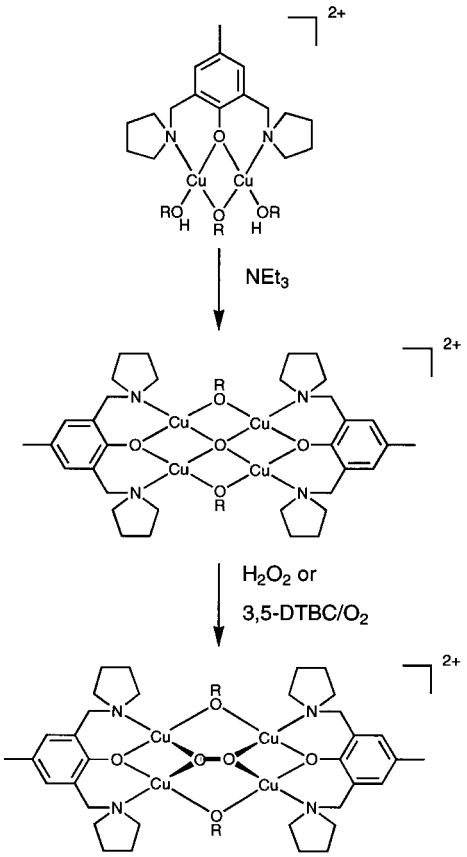

Scheme 2. Reaction of Cu_2L^1 to form tetranculear μ_4-oxo and μ_4-peroxo complex species (R = -H, -CH_3).

transitions. In methanol, hydrogen bonds may be formed with the bound peroxide group influencing the charge-transfer transitions indirectly. A combination of both effects may cause different coordination geometries of the peroxo complexes in different solvents, which would directly influence the O_2^{2-} charge-transfer transitions.

Experimental Section

Physical measurements: ^1H NMR spectra were recorded on a Bruker WH 300 instrument; all chemical shifts are reported relative to an internal standard of tetramethylsilane. Elemental analyses were performed on a Heraeus CHN-O-RAPID instrument. Electronic spectra were recorded on a Shimadzu UV-3100 spectrophotometer. The ESI-MS measurements were performed on a Finnigan MAT 95 double-focussing apparatus (BE configuration) equipped with an API II electrospray ion source (Finnigan) and on a HP 5989 Engine (single quadrupole analyzer, Hewlett – Packard) equipped with an Analytica Branford II electrospray ion source. The samples were dissolved in CH_2Cl_2 (ca. 0.5 mg mL^{-1}) and ion optics were adjusted to minimize the presence of doubly charged species. IR (solids in KBr, oils between NaCl plates) and FIR spectra (in polyethylene) were recorded on a Bruker IF 113 v spectrometer. FT Raman spectra were recorded at room temperature with pure samples on a Bruker IFS 66 FT Raman interferometer with a Nd-YAG laser excitation of 1064 nm (Adlas). Resonance Raman spectra were performed on a multichannel spectrometer XY (Dilor) and on a U 1000 Raman spectrometer (Instruments S.A.) excited with Kr^+ and Ar^+ lasers (Spectra Physics models 2025 and 165). The samples were diluted in a KBr matrix and fixed on a rotating steel disk; the spectra were measured at 10, 20 or 80 K. Magnetic susceptibilities of powdered samples of **1** and **4** were recorded on a Faraday-type magneto-

0947-6539/98/0402-0296 $ 17.50+.50/0 *Chem. Eur. J.* **1998**, *4*, No. 2

meter with a Cahn RG electrobalance in the temperature range 4.3–300 K. A similar balance was used for the temperature range 300–411.2 K. The applied magnetic field was about 1.5 T in the low temperature and about 1.2 T in the higher temperature range. Details of the apparatus have been described elsewere.[27,30] The experimental susceptibility data were corrected for diamagnetism in the usual manner with Pascal's constants.[31] Corrections for diamagnetism were estimated as -556.5×10^{-6} and -574.9×10^{-6} cm^{3}mol^{-1} for **1** and **4**, respectively.

Reagents: All reagents were purchased from commercial sources and used as received. If necessary solvents were dried by standard procedures. The gas $^{18}O_2$ (95–98% ^{18}O) was obtained from Cambridge Isotope Laboratories and used without further purification.

Synthesis of 2,6-bis(pyrrolidinomethyl)-4-methylphenol (HL^1): *p*-Cresol (5.41 g, 50 mmol) and pyrrolidine (7.82 g, 9.1 mL, 110 mmol) were dissolved in ethanol (60 mL). The solution was treated with 36% formaldehyde solution (8.8 mL, 115 mmol), stirred for 24 h under reflux and then evaporated to dryness under vacuum. The residue was washed with sodium carbonate solution (10%, 40 mL). This solution was extracted three times with ether and the combined organic phases were subsequently dried over sodium sulfate. The ether was removed under vacuum to give a light yellow oil. Yield: 11.4 g (83%); ^{1}H NMR (300 MHz, $CDCl_3$, TMS): $\delta=$ 1.80 (m, 8H), 2.59 (m, 8H), 3.70 (s, 4H), 6.85 (s, 2H); $C_{17}H_{26}N_2O$ (274.41): calcd C 74.41, H 9.55, N 10.21; found C 73.88, H 9.71, N 10.60.

Synthesis of 2,6-bis(piperidinomethyl)-4-methylphenol (HL^2): *p*-Cresol (5.41 g, 50 mmol) and piperidine (9.37 g, 10.9 mL, 110 mmol) were dissolved in dioxane (50 mL). Paraformaldehyde (3.30 g, 110 mmol) was added to this solution and the mixture was refluxed for 24 h. After evaporation of the solvent the residue was treated with sodium carbonate solution (10%, 40 mL). The solution was extracted three times with ether and the combined organic phases were dried over sodium sulfate. The ether was removed under vacuum. The resulting colourless oil crystallized slowly upon standing in a refrigerator. Yield: 13.20 g (88%); ^{1}H NMR (300 MHz, $CDCl_3$, TMS): $\delta=1.46$ (m, 4H), 1.58 (m, 8H), 2.22 (s, 3H), 2.47 (m, 8H), 3.55 (s, 4H), 6.83 (s, 2H); $C_{19}H_{30}N_2O$ (302.46): calcd C 75.45, H 10.00, N 9.26; found C 75.50, H 10.47, N 9.48.

Synthesis of 2,6-bis(morpholinomethyl)-4-methylphenol (HL^3): Morpholine (11.8 g, 11.8 mL, 135 mmol) was added to a solution of *p*-cresol (6.48 g, 60 mmol) in dioxane (30 mL). The mixture was stirred and a solution of formaldehyde (36%, 9.9 mL, 130 mmol) was added. The solution was then heated to reflux and kept at this temperature for 2 h, after which the solvent was evaporated under vacuum. The crude solid was recrystallized from toluene. Yield: 4.68 g (26%); m.p. 118 °C; ^{1}H NMR (300 MHz, [D$_6$]acetone, TMS): $\delta=2.23$ (s, 3H), 2.53 (t, 8H), 3.59 (s, 4H), 3.73 (t, 8H), 6.86 (s, 2H); $C_{17}H_{26}N_2O_3$ (306.40): calcd C 66.67, H 8.50, N 9.15; found C 67.20, H 8.80, N 9.04.

Synthesis of [Cu$_4$(L^1)$_2$(O$_2$)(OMe)$_2$(ClO$_4$)]ClO$_4$·MeOH (1): [Cu(ClO$_4$)$_2$]·6H$_2$O (185 mg, 0.50 mmol) was dissolved in methanol (30 mL). The solution was stirred and the ligand HL^1 (69 mg, 0.25 mmol) was added. After addition of NEt_3 (0.4 mL) and H_2O_2 solution (30%, 13 μL, 0.125 mmol), or alternatively 3,5-DTBC (56 mg, 0.25 mmol), dark green crystals of **1** were formed within a few hours. Yield: 60 mg (42%); $C_{37}H_{60}N_4Cl_2Cu_4O_{15}$ (1125.95): calcd C 39.47, H 5.37, N 4.98; found C 40.01, H 5.23, N 5.25.

Synthesis of [Cu$_4$(L^2)$_2$(O$_2$)(OMe)$_2$(ClO$_4$)]ClO$_4$·MeOH (2): [Cu(ClO$_4$)$_2$]·6H$_2$O (185 mg, 0.50 mmol) was dissolved in methanol (20 mL). The solution was stirred and the ligand HL^2 (76 mg, 0.25 mmol) was added. After addition of NEt_3 (0.4 mL) and 3,5-DTBC (56 mg, 0.25 mmol) **2** was obtained as a dark green microcrystalline product. Yield: 75 mg (50%); $C_{41}H_{68}N_4Cl_2Cu_4O_{15}$ (1182.11): calcd C 41.66, H 5.80, N 4.74; found C 41.93, H 6.00, N 4.66.

Synthesis of [Cu$_4$(L^3)$_2$(O$_2$)(OMe)$_2$(ClO$_4$)]ClO$_4$·MeOH (3): [Cu(ClO$_4$)$_2$]·6H$_2$O (93 mg, 0.25 mmol) was dissolved in methanol (15 mL). The solution was stirred and HL^3 (38 mg, 0.125 mmol) was added. After addition of a few drops of NEt_3 and 3,5-DTBC (56 mg, 0.25 mmol) **3** was obtained as a dark green microcrystalline product. Yield: 40 mg (54%); $C_{37}H_{60}N_4Cl_2Cu_4O_{19}$ (1189.95): calcd C 37.35, H 5.08, N 4.71; found C 36.38, H 5.05, N 4.72.

Synthesis of [Cu$_4$(L^1)$_2$(O)(OH)$_2$(MeOH)$_2$(ClO$_4$)$_2$] (4): [Cu(ClO$_4$)$_2$]·6H$_2$O (371 mg, 1.00 mmol) was dissolved in methanol (5 mL). HL^1 (137 mg, 0.50 mmol) was added in small portions under stirring. NEt_3 (1 mL) was added and the mixture was allowed to stand for one day, after which small amounts of precipitate were filtered off. $NaClO_4$ (200 mg, 1.63 mmol) was added to this solution. Dark green crystals were formed after a few hours. Yield: 80 mg (29%); $C_{36}H_{60}N_4Cl_2Cu_4O_{15}$ (1113.94): calcd C 38.83, H 5.43, N 5.03; found C 38.33, H 5.30, N 5.15.

Crystal structure determination: Intensity data of complex **1** were collected on a Syntex P2$_1$ four-circle diffractometer ($Mo_{K\alpha}$, $\lambda=0.71073$ Å, graphite monochromator) with the ω-scan technique with a variable scan rate of 2.93–29.30° min^{-1}. The intensities of two reflections were monitored; no significant crystal deterioration was observed. Intensity data of complex **4** were collected on a STOE IPDS diffractometer ($Mo_{K\alpha}$, $\lambda=0.71073$ Å, graphite monochromator) with a sample-to-plate distance of 70 mm and a scan range from 0 to 180° with an exposure time of 3 min per 3° increment. A combined absorption and decay correction was applied (program DECAY[32]). Further data collection parameters are summarized in Table 1. The structures were solved by Patterson syntheses (program XS[33]). A series of full-matrix least-squares refinement cycles on F^2 (program SHELXL 93[34]) followed by Fourier syntheses gave all remaining atoms. The hydrogen atoms were placed at calculated positions and were constrained to ride on the atom to which they are attached. The isotropic thermal parameters for the methyl and hydroxyl protons were refined with 1.5 times the U_{eq} value of the corresponding atom and for all other hydrogen atoms with 1.2 times U_{eq}. The non-hydrogen atoms were refined with anisotropic thermal parameters. In **1** the oxygen atom of the disordered methanol molecule (C19–O4) was refined with an occupancy factor of 0.5 because the bound carbon atom is located on a twofold axis. In **4** occupancy factors of 0.69(3) for O4 and 0.31(3) for (O4′) were found for the disordered methanol molecule. Hydrogen atoms for C18–O4′ were not calculated.

Crystallographic data (excluding structure factors) for the structures reported in this paper have been deposited with the Cambridge Crystallographic Data Centre as supplementary publication no. CCDC-100661. Copies of the data can be obtained free of charge on application to CCDC, 12 Union Road, Cambridge CB2 1EZ, UK (Fax: Int. code +(44) 1223 336-033; e-mail: deposit@ccdc.cam.ac.uk).

Spectrophotometric titrations: A solution containing HL^1 (2×10^{-4} mol L^{-1}) and [Cu(ClO$_4$)$_2$]·6H$_2$O (4×10^{-4} mol L^{-1}) in methanol (2 mL) was titrated with a solution of NEt_3 (0.1M) in methanol. After each addition thermodynamic equilibrium was reached instantaneously. The UV/Vis spectra were corrected for volume changes.

A solution of triethylamine (0.1M, 120 μL, 30 equivalents with respect to Cu$_2$ unit) in methanol was added to a solution containing HL^1 (2×10^{-4} mol L^{-1}) and [Cu(ClO$_4$)$_2$]·6H$_2$O (4×10^{-4} mol L^{-1}) in methanol (2 mL). This solution was titrated with a solution of H_2O_2 (0.01M). After each addition thermodynamic equilibrium was reached instantaneously. No decomposition of H_2O_2 was observed, the spectra of each titration step remained constant for at least one hour. The UV/Vis spectra were corrected for volume changes.

Acknowledgements: Financial support from the Deutsche Forschungsgemeinschaft, the Fonds der Chemischen Industrie and the VW-Stiftung is gratefully acknowledged. We thank Prof. Dr. H. Homborg (Christian-Albrechts-Universität Kiel) for recording the Raman spectra and Dr. D. Stöckigt (Max-Planck-Institut für Kohlenforschung, Mülheim) for measuring the ESI-MS spectra.

Received: September 1, 1997 [F809]

[1] For recent reviews see: a) W. Kaim, J. Rall, *Angew. Chem.* **1996**, *108*, 47–64; *Angew. Chem. Int. Ed. Engl.* **1996**, *35*, 43–60; b) N. Kitajima, Y. Moro-oka, *Chem. Rev.* **1994**, *94*, 737–757; c) E. I. Solomon, F. Tuczek, D. E. Root, C. A. Brown, *ibid.* **1994**, *94*, 827–856; d) K. D. Karlin, Z. Tyeklár, A. D. Zuberbühler, in *Bioinorganic Catalysis* (Ed.: J. Reedijk), Marcel Dekker, New York, Basel, Hong Kong, **1993**, pp. 261–315; e) N. Kitajima, *Adv. Inorg. Chem.* **1992**, *38*, 1–77.

[2] a) J. S. Thompson, *J. Am. Chem. Soc.* **1984**, *106*, 4057–4059; b) J. S. Thompson, *ibid.* **1984**, *106*, 8308–8309; c) N. J. Blackburn, R. W. Strange, R. W. Cruse, K. D. Karlin, *ibid.* **1987**, *109*, 1235–1237; d) J. E. Pate, R. W. Cruse, K. D. Karlin, E. I. Solomon, *ibid.* **1987**, *109*, 2624–2630; e) K. D. Karlin, R. W. Cruse, Y. Gultneh, A. Farooq, J. C. Hayes, J. Zubieta, *ibid.* **1987**, *109*, 2668–2679; f) T. N. Sorrell, V. A.

Vankai, *Inorg. Chem.* **1990**, *29*, 1687 – 1692; g) R. W. Cruse, S. Kaderli, K. D. Karlin, A. D. Zuberbühler, *J. Am. Chem. Soc.* **1988**, *110*, 6882 – 6883; h) K. D. Karlin, N. Wei, B. Jung, S. Kaderli, P. Niklaus, A. D. Zuberbühler, *ibid.* **1993**, *115*, 9506 – 9514; i) B. Jung, K. D. Karlin, A. D. Zuberbühler, *ibid.* **1996**, *118*, 3763 – 3764.

[3] K. Fujisawa, M. Tanaka, Y. Moro-oka, N. Kitajima, *J. Am. Chem. Soc.* **1994**, *116*, 12079 – 12080.

[4] a) R. R. Jacobson, Z. Tyeklár, A. Farooq, K. D. Karlin, S. Liu, J. Zubieta, *J. Am. Chem. Soc.* **1988**, *110*, 3690 – 3692; b) Z. Tyeklár, R. R. Jacobson, N. Wei, N. N. Murthy, J. Zubieta, K. D. Karlin, *ibid.* **1993**, *115*, 2677 – 2689.

[5] a) N. Kitajima, K. Fujisawa, Y. Moro-oka, K. Toriumi, *J. Am. Chem. Soc.* **1989**, *111*, 8975 – 8976; b) N. Kitajima, K. Fujisawa, C. Fujimoto, Y. Moro-oka, S. Hashimoto, T. Kitagawa, K. Toriumi, K. Tatsumi, A. Nakamura, *ibid.* **1992**, *114*, 1277 – 1291.

[6] a) K. A. Magnus, B. Hazes, H. Ton-That, C. Bonaventura, J. Bonaventura, W. G. J. Hol, *Proteins: Struct. Funct. Genet.* **1994**, *19*, 302 – 309; b) K. A. Magnus, H. Ton-That, J. E. Carpenter, *Chem. Rev.* **1994**, *94*, 727 – 735; c) T. B. Freedman, J. S. Loehr, T. M. Loehr, *J. Am. Chem. Soc.* **1976**, *98*, 2809 – 2815; d) R. S. Himmelwright, N. C. Eickman, C. D. LuBien, E. I. Solomon, *ibid.* **1980**, *102*, 5378 – 5388.

[7] a) M. Mahroof-Tahir, N. N. Murthy, K. D. Karlin, N. J. Blackburn, S. N. Shaikh, J. Zubieta, *Inorg. Chem.* **1992**, *31*, 3001 – 3003; b) J. E. Bol, W. L. Driessen, R. Y. N. Ho, B. Maase, L. Que, Jr., J. Reedijk, *Angew. Chem.* **1997**, *109*, 1022 – 1025; *Angew. Chem. Int. Ed. Engl.* **1997**, *36*, 998 – 1000; c) K. D. Karlin, Dong-Heon Lee, S. Kaderli, A. D. Zuberbühler, *Chem. Commun.* **1997**, 475 – 476.

[8] J. Reim, B. Krebs, *Angew. Chem.* **1994**, *106*, 2040 – 2041; *Angew. Chem. Int. Ed. Engl.* **1994**, *33*, 1969 – 1971.

[9] J. H. Hodgkin, *Aust. J. Chem.* **1984**, *37*, 2371 – 2378.

[10] W. Micklitz, S. G. Bott, J. G. Bentsen, S. J. Lippard, *J. Am. Chem. Soc.* **1989**, *111*, 372 – 374.

[11] R. Stomberg, L. Trysberg, I. Larking, *Acta Chem. Scand.* **1970**, *24*, 2678 – 2679.

[12] I. Shweky, L. E. Pence, G. C. Papaefthymiou, R. Sessoli, J. W. Yun, A. Bino, S. J. Lippard, *J. Am. Chem. Soc.* **1997**, *119*, 1037 – 1042.

[13] H. J. Breunig, T. Krüger, E. Lork, *Angew. Chem.* **1997**, *109*, 654 – 655; *Angew. Chem. Int. Ed. Engl.* **1997**, *36*, 615 – 617.

[14] a) J. G. Bentsen, W. Micklitz, S. Bott, S. J. Lippard, *J. Inorg. Biochem.* **1989**, *36*, 226; b) D. M. Proserpio, R. Hoffmann, G. C. Dismukes, *J. Am. Chem. Soc.* **1992**, *114*, 4374 – 4382.

[15] A. Gelasco, A. Askenas, V. L. Pecoraro, *Inorg. Chem.* **1996**, *35*, 1419 – 1420.

[16] A. L. Feig, M. Becker, S. Schindler, R. van Eldik, S. J. Lippard, *Inorg. Chem.* **1996**, *35*, 2590 – 2601.

[17] J. A. Samuels, Wen-C. Chiang, J. C. Huffman, K. L. Trojan, W. E. Hatfield, D. V. Baxter, K. G. Caulton, *Inorg. Chem.* **1994**, *33*, 2167 – 2179.

[18] V. McKee, S. S. Tandon, *J. Chem. Soc. Dalton Trans.* **1991**, 221 – 230.

[19] Recent examples: a) J. Reim, K. Griesar, W. Haase, B. Krebs, *J. Chem. Soc. Dalton Trans.* **1995**, 2649 – 2656; b) S. Teipel, K. Griesar, W. Haase, B. Krebs, *Inorg. Chem.* **1994**, *33*, 456 – 464; c) L. Chen, S. R. Breeze, R. J. Rousseau, S. Wang, L. K. Thompson, *ibid.* **1995**, *34*, 454 – 465; d) T. Kogane, T. Yamamoto, M. Hayashi, R. Hirota, C. A. Horiuchi, *Polyhedron* **1995**, *14*, 2475 – 2482; e) A. J. Blake, C. M. Grant, C. I. Gregory, S. Parsons, J. M. Rawson, D. Reed, R. E. P. Winpenny, *J. Chem. Soc. Dalton Trans.* **1995**, 163 – 175; f) F. S. Keij, J. G. Haasnoot, A. J. Oosterling, J. Reedijk, C. J. O'Connor, J. H. Zang, A. L. Spek, *Inorg. Chim. Acta* **1991**, *181*, 185 – 193; g) H. M. Haendler, *Acta Crystallogr.* **1990**, *C46*, 2054 – 2057; h) A. Erdonmez, J. H. van Diemen, R. A. G. de Graaff, J. Reedijk, *ibid.* **1990**, *C46*, 402 – 404.

[20] E. I. Solomon, F. Tuczek, D. E. Root, C. A. Brown, *Chem. Rev.* **1994**, *94*, 827 – 856.

[21] B. J. Hathaway, *Struct. Bonding* **1984**, *57*, 55 – 118.

[22] a) N. Kitajima, T. Koda, S. Hashimoto, T. Kitagawa, Y. Moro-oka, *J. Chem. Soc. Chem. Commun.* **1988**, 151 – 152; b) N. Kitajima, T. Koda, S. Hashimoto, T. Kitagawa, Y. Moro-oka, *J. Am. Chem. Soc.* **1991**, *113*, 5664 – 5671.

[23] a) J. S. Loehr, T. B. Freedman, T. M. Loehr, *Biochem. Biophys. Res. Commun.* **1974**, *56*, 510 – 515; b) T. J. Thamann, J. S. Loehr, T. M. Loehr, *J. Am. Chem. Soc.* **1977**, *99*, 4187 – 4189; c) J. A. Larrabee, T. G. Spiro, N. S. Ferris, W. H. Woodruff, W. A. Maltese, M. S. Kerr, *ibid.* **1977**, *99*, 1979 – 1980; d) J. A. Larrabee, T. G. Spiro, *ibid.* **1980**, *102*, 4217 – 4223; e) J. Ling, L. P. Nestor, R. S. Czernuszewicz, T. G. Spiro, R. Fraczkiewicz, K. D. Sharma, T. M. Loehr, J. Sanders-Loehr, *ibid.* **1994**, *116*, 7682 – 7691; f) H. S. Mason, W. L. Fowlks, E. Peterson, *ibid.* **1955**, *77*, 2914 – 2915.

[24] M. J. Baldwin, P. K. Ross, J. E. Pate, Z. Tyeklár, K. D. Karlin, E. I. Solomon, *J. Am. Chem. Soc.* **1991**, *113*, 8671 – 8679.

[25] J. E. Pate, R. W. Cruse, K. D. Karlin, E. I. Solomon, *J. Am. Chem. Soc.* **1987**, *109*, 2624 – 2630.

[26] B. Bleaney, K. D. Bowers, *Proc. R. Soc. London Ser. A* **1952**, *214*, 451.

[27] L. Merz, W. Haase, *J. Chem. Soc. Dalton Trans.* **1980**, 875 – 879.

[28] a) V. H. Crawford, H. W. Richardson, J. R. Wasson, D. J. Hodgson, W. E. Hatfield, *Inorg. Chem.* **1976**, *15*, 2107 – 2110; b) M. Handa, N. Koga, S. Kida, *Bull. Chem. Soc. Jap.* **1988**, *61*, 3853 – 3857; c) L. K. Thompson, S. K. Mandal, S. S. Tandon, J. N. Bridson, M. K. Park, *Inorg. Chem.* **1996**, *35*, 3117 – 3125; d) J. Lorösch, U. Quotschalla, W. Haase, *Inorg. Chim. Acta* **1987**, *131*, 229 – 236; e) R. Fletcher, J. J. Hansen, J. Livermore, R. D. Willett, *Inorg. Chem.* **1983**, *22*, 330 – 334.

[29] K. D. Karlin, Z. Tyeklár, A. Farooq, R. R. Jacobson, E. Sinn, D. W. Lee, J. E. Bradshaw, L. J. Wilson, *Inorg. Chim. Acta* **1991**, *182*, 1 – 3.

[30] S. Gehring, P. Fleischhauer, H. Paulus, W. Haase, *Inorg. Chem.* **1993**, *32*, 54 – 60.

[31] O. Kahn, *Molecular Magnetism*, VCH, New York, **1993**.

[32] STOE IPDS software package, STOE & CIE, Darmstadt, **1993**.

[33] G. M. Sheldrick, *SHELXTL PLUS*, Siemens Analytical X-ray Instruments, Madison, WI, **1990**.

[34] G. M. Sheldrick, *SHELXL 93, Program for Crystal Structure Determinations*, University of Göttingen, **1993**.

0947-6539/98/0402-0298 $ 17.50+.50/0 *Chem. Eur. J.* **1998**, *4*, No. 2